Towards Radar-Enabled Sensor Networks

Prabal K. Dutta
EECS Department
Univ. of California, Berkeley
Berkeley, California 94720
prabal@cs.berkeley.edu

Anish K. Arora
CSE Department
The Ohio State University
Columbus, Ohio 43210
anish@cse.osu.edu

Steven B. Bibyk
ECE Department
The Ohio State University
Columbus, Ohio 43210
bibyk@ece.osu.edu

ABSTRACT

Ultrawideband radar-enabled wireless sensor networks have the potential to address key detection and classification requirements common to many surveillance and tracking applications. However, traditional radar signal processing techniques are mismatched with the limited computational and storage resources available on typical sensor nodes. The mismatch is exacerbated in noisy, cluttered environments or when the signals have corrupted spectra. To explore the compatibility of ultrawideband radar and mote-class sensor nodes, we designed and built a new platform called the *Radar Mote*. An early prototype of this platform was used to detect, classify, and track people and vehicles moving through an outdoor sensor network deployment. This paper describes the sensor's theory of operation, discusses the design and implementation of the Radar Mote, and presents sample signal waveforms of people, vehicles, noise, and clutter. We demonstrate that radar sensors can be successfully integrated with mote-class devices and imbue them with an extraordinarily useful sensing modality.

Categories and Subject Descriptors

C.0 [**General**]: Hardware/Software Interfaces; C.3 [**Special-Purpose and Application-Based Systems**]: Signal Processing Systems; G.3 [**Probability and Statistics**]: Time Series Analysis; J.7 [**Computers in Other Systems**]: Military

General Terms

Measurement, Design, Experimentation

Keywords

Sensor Networks, Intrusion Detection, Surveillance, Radar, Ultrawideband Radar, Micropower Impulse Radar, Detection, Classification, Signal Processing

IPSN'06, April 19–21, 2006, Nashville, Tennessee, USA.

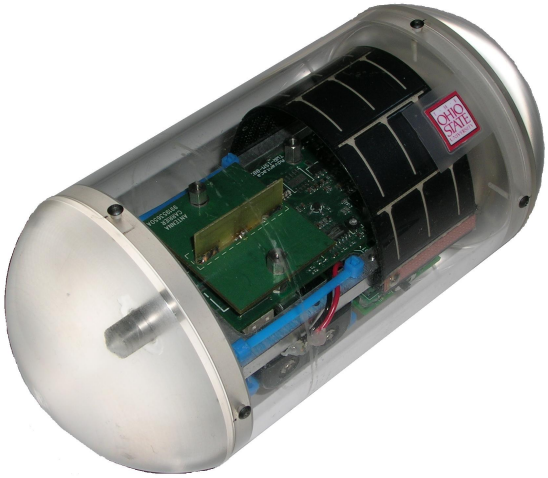

Figure 1: The Radar Mote: An ultrawideband radar-enabled wireless sensor network node.

1. INTRODUCTION

Historically, surveillance systems have used infrared, acoustics, seismic, and magnetics for passive sensing, and optics and ultrasonics for active sensing, but radar has been conspicuously absent. Conventional radio detection and ranging (radar) systems employ transmitted and reflected microwaves to detect, locate, and track objects over long distances and large areas. Due to its versatility, radar has found applications in defense, law enforcement, meteorology, and mapping. However, widespread commercial applications of radar have been limited because conventional systems are expensive, bulky, and difficult to use. Two exceptions are motion sensors which have a short range and poor false alarm rates when co-located or used in unstructured environments, and police radar which employ a focused, high-power beam. Since many sensor networks operate in unstructured environments with limited energy supplies, these conventional sensors are unsuitable for sensor networks.

A new kind of radar sensor system based on time domain reflectometry (TDR) techniques and ultrawideband (UWB) technology was developed in the mid-1990s at Lawrence Livermore National Labs [5]. These new radar sensors use micropower impulses rather than continuous narrowband transmissions and are inexpensive, compact, and low-power. These sensors offer detection, ranging, and velocimetry ca-

pabilities, which make them ideal for use with wireless sensor networks. UWB radar, like conventional radar, uses transmitted and reflected microwaves. However, unlike conventional systems that transmit bursts of narrowband continuous waves, UWB uses very short, and consequently ultrawideband, pulses. These short pulses contain very little energy but since the energy they do contain is spread across a broad range of frequencies, UWB signals are better able to penetrate obstacles and are more immune to multipath effects. Due to its many benefits over conventional radar, UWB radar technology is being increasingly adopted in systems like proximity detectors, motion sensors, rangefinders, electronic dipsticks, graphics tablets, stud finders, and tripwires. For the remainder of this work, we will use the term *UWB radar* or simply *radar* when referring to ultrawideband radar sensors which operate on this principle. Section 2 outlines the basic theory behind the sensors we used.

In Section 3, we present the *Radar Mote*, a new sensor network platform for detecting moving objects like people and vehicles. The Radar Mote, shown in Figure 1, integrates an Advantaca ultrawideband (UWB) radar sensor, a Mica2 mote, an (optional) Mica sensor board, and a custom power board. These circuit boards are housed in a self-righting enclosure that ensures the radar's antenna is always oriented vertically. A network of twelve Radar Motes were used in a surveillance application to successfully detect, classify, and track people and vehicles moving through a sensor field [2].

One of the challenges when considering a new sensing modality is understanding the underlying sensing model. A sensor's theory of operation provides a mathematical description of how the sensor works but because of the wide range of variables in any actual deployment, it is often more useful to visualize actual sensor signal traces due to various targets and environments. In Section 4, representative signal traces are presented for a person walking and running, a vehicle driving, and several noisy environments.

Detection is process of discriminating a signal of interest from the background noise of the environment and the clutter noise from other objects that are not of interest. Signal processing algorithms for detection can range from simple threshold detectors to much more complex signal processing networks. For our experiments, we used a simple, binary-hypothesis, Neyman-Pearson detector that runs on mote-class devices. The detector logic, and the result of it running over sample signal traces, is presented in Section 5.

As an active rather than passive technology, UWB radar has a larger sensing radius than either infrared or magnetic sensors and consequently UWB radar can be deployed in lower densities. UWB radar sensors require neither line-of-sight like infrared sensors nor exposure to the environment like acoustic sensors, making them easy to conceal inside of trees, rocks, or other objects which are impervious to light and sound. For foot traffic, UWB and seismic sensors offer similar sensing range but unlike seismic sensors, UWB radars do not need to be staked into the ground. UWB radars are active sensors since they transmit short bursts of RF energy but since their transmissions are very short, the pulses usually appear to be background noise. The sensors can be made both difficult to detect and resistant to jamming by dithering the pulse repetition rate or using other coding techniques. Section 6 places radar in the larger context of experimental sensor networks for intrusion detection and the sensors that those networks use.

2. THEORY OF OPERATION

Ultrawideband radar is available in two broad categories: pulse Doppler and pulse echo. Pulse Doppler radar operates on the Doppler principle and is primarily used for motion sensing. Pulse echo radar employs time-of-flight and is typically used as a rangefinder. For this work, we use pulse Doppler radar sensors. Consequently, for the remainder of this work, when we refer to UWB radar, we mean pulse Doppler radar unless explicitly stated otherwise.

UWB radar works by transmitting a short pulse and detecting its reflection. If the object that reflects the transmitted pulse is moving, then the frequency of the reflected pulse will be Doppler-shifted to a frequency that is slightly different from the transmitted pulse. The reflected pulse with frequency f' is related to the transmitted pulse with frequency f through the familiar Doppler equation

$$f' = f\left(\frac{c}{c \pm v_o}\right) \tag{1}$$

where c is the speed of light, v_o is the speed of the object, and $\pm$ is chosen such that $f' > f$ when the object is moving toward the sensor. An UWB radar does not wait indefinitely for a reflection. Rather, the system waits a configurable period of time. This period corresponds to the maximum round-trip time of the signal, which in turn implies a distance or "range gate" outside of which objects are not detected.

An UWB radar mixes the transmitted and reflected pulses in a manner that computes the difference, Δf, between these two signals. This difference results in the familiar beat frequency that arises when two nearby frequencies mix. This signal is usually capacitively coupled to eliminate bias and low pass filtered to eliminate high frequency components due to fast-moving objects. In essence, the signal is band-limited to the range of frequencies that correspond to the range of valid v_o values for our objects of interest. This filtered signal is made available through an analog output port on the radar.

The output of the mixer, Δf, is the difference between the transmitted and reflected frequencies

$$\Delta f = f - f' \tag{2}$$

which can be written

$$\Delta f = f\left(1 - \frac{c}{c \pm v_o}\right) \tag{3}$$

rearranging to solve for v_o and simplifying gives

$$v_o = \pm c\left(\frac{\Delta f}{f - \Delta f}\right) \tag{4}$$

Since we know c and f, if we can measure Δf, then we can also determine v_o. For example, if an UWB radar with a 2.4GHz center frequency outputs a signal with Δf =16Hz, an object would be moving with a radial velocity of 2m/s.

We can further simplify the computation by recognizing that for the objects of interest to us, $\Delta f << f$, so

$$v_o = \pm c\left(\frac{\Delta f}{f - \Delta f}\right) \tag{5}$$

becomes

$$v_o \approx \pm c\left(\frac{\Delta f}{f}\right) \tag{6}$$

and a signal's wavelength $\lambda = c/f$ gives

$$v_o \approx \pm \Delta f \lambda \quad (7)$$

and a signal's period $\Delta T = 1/\Delta f$ gives

$$v_o \approx \pm \lambda / \Delta T \quad (8)$$

A sinusoidal signal encounters a zero-crossing every $\Delta T_z = \Delta T/2$, which corresponds to half of a wavelength. In principle, estimating ΔT_z is a matter measuring the elapsed time between successive zero crossings.

In addition to the target object, the transmitted pulse is reflected or "scattered" by other nearby objects like rocks, trees, and walls which are of no interest. These useless reflections are called clutter. The strength of a reflection is a function of an object's shape, size, permittivity, and permeability. Fortunately, most of the objects that cause clutter are stationary and their reflections, no matter how strong, are filtered out. Therefore, in theory, the beat frequency due to clutter is zero and the sensor's analog output is a constant voltage. However, in practice, we find that some background noise (e.g. due to the environmental or thermal noise) and clutter noise (e.g. due to a leaf fluttering in the wind) do have an effect on the sensor's output. Some of this noise is also filtered out but some of it is not. Distinguishing between noise and a signal of interest due to a legitimate object is the topic of detection.

3. SENSOR PLATFORM

The Radar Mote consists of several circuit boards including a main processor/radio board, an optional sensor board, an ultrawideband radar motion sensor, and a power board, as shown in Figure 2. The main board is the familiar Mica2 mote, a derivative of the Mica family of motes [10]. The motes run the TinyOS operating system [9] and are programmed using the NesC language [6]. The optional sensor board is the popular Mica Sensor Board, which includes a 2-axis magnetometer, 2-axis accelerometer, microphone, thermistor, photosensor, and sounder. The radar sensor board and power board are described in greater detail in the remainder of this section.

3.1 Radar Sensor and Antenna

We used the TWR-ISM-002 sensor available from Advantaca [1] as our radar sensor platform. This sensor detects motion up to a 20 meter radius around the sensor but this range is adjustable to a shorter distance using an onboard potentiometer. The sensor includes a 51-pin connector designed to interface mechanically with the expansion connector on the Mica Motes [10]. The sensor requires 3.4V - 6.0V (nominally 3.6V) and draws less than 1mA from this supply. The unit also requires a precise power source to provide 5.5V with a $\pm 1\%$ tolerance and draws a nominal 7.5mA from this second supply.

The sensor provides a fast-attack and slow-decay digital output meaning that the output is asserted immediately after detecting a target but is not unasserted until approximately one second after the target is no longer detected. The sensitivity, like the range, can be adjusted using a potentiometer. Adjusting the sensitivity simply varies the detection threshold used for the digital output. We found the sensor's digital output had a high false alarm rate outdoors even though indoors, the digital output performed quite well.

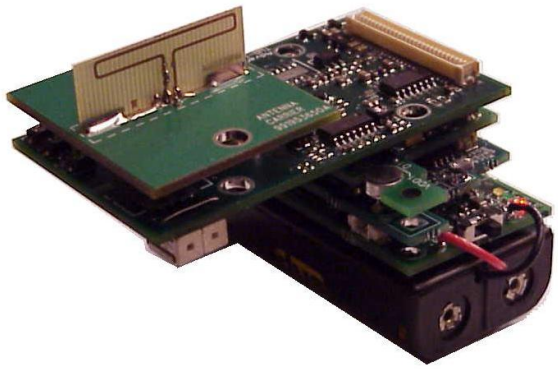

Figure 2: Radar sensor network node electronics. The circuit boards from top to bottom are: (*i*) dipole antenna for transceiving the radar signal, (*ii*) radar sensor, (*iii*) interface/power board, (*iv*) generic sensor board, and (*v*) processor/radio board. The battery case which holds two AA batteries can be seen at the bottom of the stack.

In addition to the digital output, an analog output is available. The analog output is a lowpass-filtered version of the Doppler baseband signal. The lowpass filter response has a 3 dB/octave drop-off above 18 Hz and an additional 12 dB/octave above 220 Hz. The analog output signal varies from 0V to 2.5V and is nominally biased at 1.25V when there is no motion. When a target is moving within sensing range and with a radial velocity component, the analog output oscillates between 0V and 2.5V. The output is a noisy, potentially clipped, weighted sum of sinusoids whose frequencies are related to the radial velocity of each reflecting surface (e.g. chest, arms, legs, etc.) and whose amplitude is related to the strength of the reflection. Since our application required robust detection outdoors, we used the analog output and digitally processed the signals using the detection and estimation algorithms presented in this work.

The sensor includes a dipole antenna board which mounts on top of the radar sensor board using an MMCX connector. A null in the antenna pattern makes the radar sensor vulnerable to false negatives when a target moves along the antenna's (and node's) lengthwise axis. The spherical radiation pattern of the dipole antenna is a poor choice for embedded surveillance applications because a considerable amount of signal power is directed downward. Discone or other antennas that radiate slightly upward or even more horizontally may be a better choice for some applications.

3.2 Mica Power Board

Despite the mechanical compatibility through the expansion connector interface, matching signal pin assignments, and common power pin assignments between the radar sensor and the Mica mote, the radar does require different and incompatible operating voltages. The Mica motes require, and through the expansion connector provide, the raw battery voltage which can vary from 3.3V nominally to 2.7V.

Since the supply voltages required by the radar sensor board exceed the voltages and tolerances provided by the our batteries, we designed a circuit consisting of a pair of boost

switching regulators to generate these higher voltages and provide the necessary tolerances. The Mica Power Board implements this circuit and is shown in Figure 3. The board owes its odd footprint with a U-shaped cutout in the upper left and a square with rounded corners in the middle to a desire to maintain physical compatibility with the existing Mica Sensor Board.

Figure 3: The Mica Power Board has two fully independent switching regulators that are potentiometer adjustable and can deliver 3V - 40V at 200mA each. The odd shape of this board is reflects the need for physically compatibility with the Mica Sensor Board.

The Mica Power Board has two fully independent switching regulators that are potentiometer adjustable and can deliver 3V - 40V at 200mA each. The circuit works by intercepting the two power signals available through the bottom expansion connector and replacing these signals with the outputs of the two regulators and then passing the regulator output through the top connector. The Mica Power Board also includes a shutdown feature. When the board is in the shutdown state, power is simply passed though the board as if it were not present.

3.3 Packaging

Sensor nodes for surveillance applications may experience diverse and hostile environments with wind, rain, snow, flood, heat, cold, terrain, and canopy. The sensor packaging is responsible for protecting the delicate electronics from these elements. In addition, the packaging can affect the quality of sensing and communications processes.

Our enclosure is smooth and capsule shaped, as shown in Figure 1. This shape provides a self-righting capability and minimizes wind-resistance. Earlier experiences led us to realize that wind-induced motion of the sensor itself could cause false alarms. The enclosure body was made clear to allow sunlight to pass through and illuminate a solar cell. The final design, however, does not use solar power. The sensor electronics are mounted on an aluminum frame that is attached to the capsule-shaped body using a gimbal mechanism. The gimbal is free to rotate along the long axis of the enclosure. The frame is asymmetrically weighted in favor of the side with batteries. The gimbal mechanism and rotational degree-of-freedom of the cylindrical enclosure (i.e. the enclosure "rolls"), increase the likelihood that the radar and radio antennas' plane will be perpendicular to the ground and the solar cell will be pointing toward the sky, helping to increase the node's sensing range, communications range, and lifetime.

4. SENSOR TRACES

This section presents sample signal traces of a person walking and running by the radar, a vehicle driving past the radar, and the noise and clutter of various outdoor environments. Figures 4 and 5 show normalized,[1] zero-mean signal traces and spectrograms of a person walking and running, respectively, past the Radar Mote with near constant speed and heading.

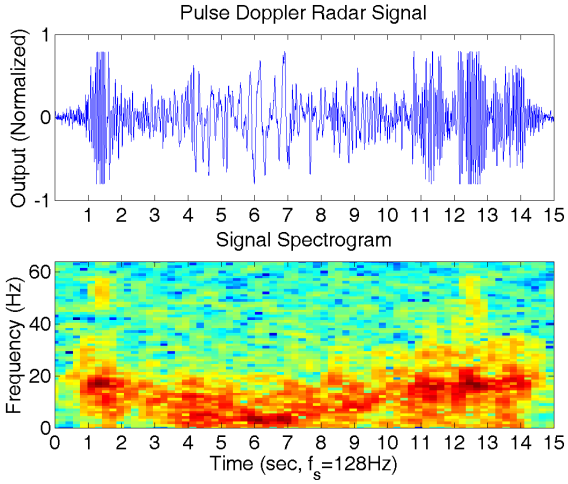

Figure 4: The radar signal and spectrogram of a walking person.

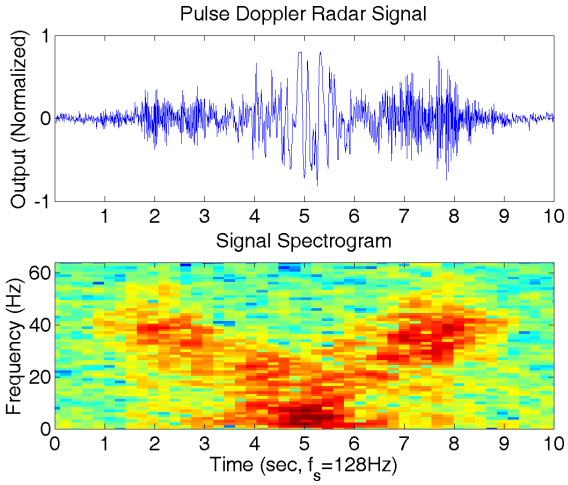

Figure 5: The radar signal and spectrogram of a running person.

When a person first comes into range of the radar, we see a signal dominated by higher frequency components. As the person gets closer to the radar, the radial velocity decreases, following a hyperbolic curve. At the person's closest point-of-approach (CPA) to the radar, the radial velocity approaches zero, assuming a non-zero CPA (i.e. the person does not walk directly over the sensor). At this point, lower

[1]Relative to the full ADC range.

frequency components dominate the power spectrum. Then, as the person moves away from the sensor, essentially the mirror image of the first half of the waveform is repeated. This waveform is typical for a constant velocity (speed and heading) trajectory.

Figure 6 shows the signal trace and spectrogram of a vehicle driving past the Radar Mote. Even though a characteristic hyperbolic signature is visible, the spectrogram of this signal has considerable power at high frequencies. Since the radar signal amplitude is related to the amount of energy reflected from the target, and the because a vehicle's large metallic body reflects far greater energy thant a human body, the radar's circuitry generates a large amplitude signal. The output of radar, however, is limited to the range of 0 - 2.5V and any signals outside of that range are clipped. These clipped signals have wideband spectra, as can be seen in Figure 6. The clipped signals and the resulting wideband spectra can create special challenges for signal processing.

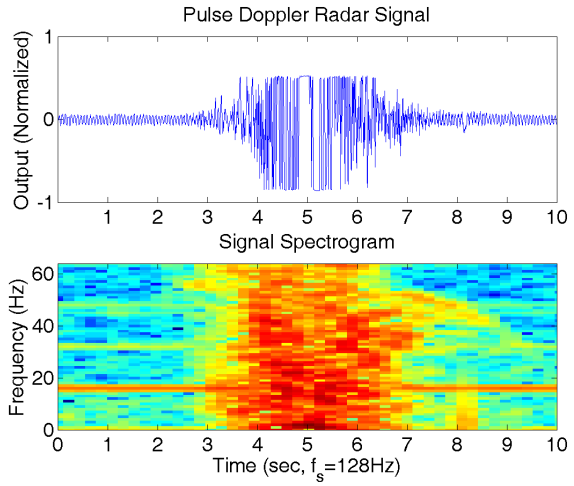

Figure 6: The radar signal and spectrogram of a passing vehicle. Note that the signal is clipped, resulting a wideband spectra.

Figure 7 shows the observed noise at several different times and locations. Background noise tends to be normally distributed and wide sense stationary over time constants larger than the time constant of a typical passing object. However, background noise may not be wide sense stationary over much larger timescales due, for example, to solar or meteorological effects. Occasionally, however, noise is not independent and identically distributed. That is, we find the occasional presence correlated of noise. This is particularly true for clutter noise due to a fluttering leaf, a flying bird, or heavy rainfall, for example, and it is more difficult to discriminate such clutter noise from signals caused by the motion of legitimate targets of interest.

Wind can affect sensors and cause a flurry of false alarms by directly moving the sensor or indirectly by moving nearby objects like grass, bushes, and trees. Since the probability of false alarm, or P_{FA}, is an important system performance metric, it is important to engineer the sensors and signal processing to withstand wind gusts and their attendant effects on the nearly environment. Similarly, rain can adversely affect both sensing and signal propagation.

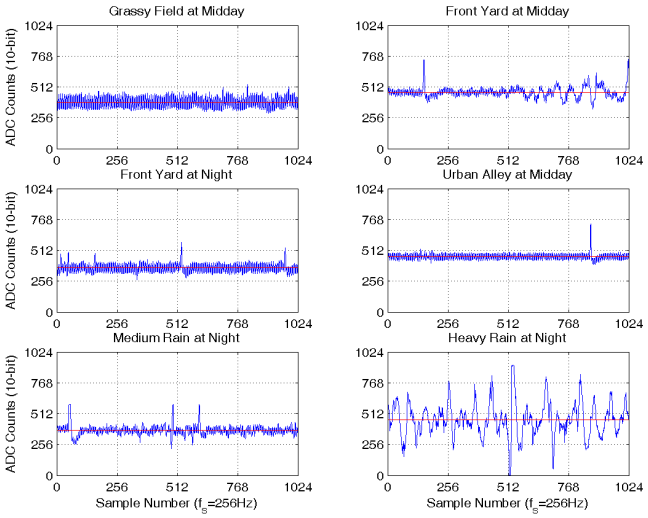

Figure 7: Sample radar noise data collected at various times and locations demonstrates the variability in the noise. The red line is the estimated bias, computed as the mean of the data set.

In the time domain, which is what we are often practically limited to on mote-class processors, the main differences between clutter and objects of interest are that clutter sometimes has a lower energy content (the signal amplitude is smaller) and frequently tends to be more bursty (lasts for a shorter period of time than legitimate targets) but occasionally tends to far less bursty (lasts for a longer period of time than a legitimate target).

5. DETECTION

In this section, we briefly outline the signal processing algorithms we used to detect the presence and motion of people and vehicles. Our algorithms are simple but effective for normal operation although they can exhibit false positives for correlated noise. The purpose of this section is to highlight some simple signal processing algorithms that work with the Radar Mote but signal processing is *not* the point of this paper. Its inclusion merely serves to highlight some possible approaches for processing radar signals.

We used a binary-hypothesis Neyman-Pearson detector to discriminate between noise (H_0) and a signal of interest (H_1). Since the background noise varies over large timescales, a constant false alarm rate (CFAR) detector is used to provide an adaptive decision threshold. Figure 8 shows several of the signal processing stages and the remainder of this section details the steps taken to transform the raw ADC signal to a detection decision.

First, the signal bias is removed. Second, the unbiased signal is normalized. Third, the magnitude of the normalized signal is computed. Fourth, the magnitude is filtered using an exponentially-weighted moving average (EWMA), which is our test statistic, X. Fifth, the signal magnitude is filtered using a second, slower-moving EWMA, which estimates the background, Y. Sixth, the magnitude is squared to compute its energy, E. Seventh, the energy is filtered using a third EWMA whose parameters are identical to the background

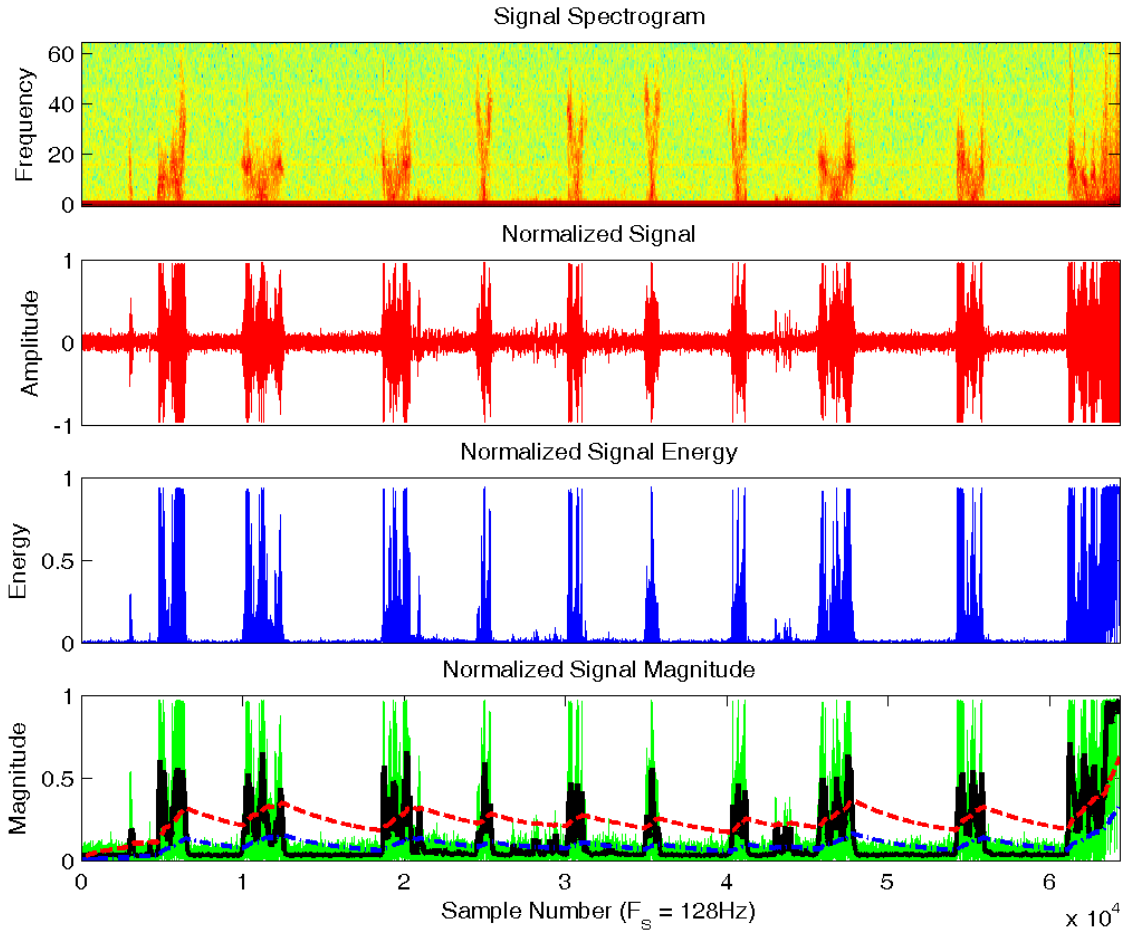

Figure 8: This figure shows the radar signal traces resulting from the three walking passes of a person followed by four running passes, followed by three more walking passes (the last of which was to pick up the sensor). The four subplots show various degrees of processing: (a) A spectrogram of the radar signal; (b) An unbiased and normalized representation of the signal; (c) The energy level of the signal; and (d) The test statistic X (solid black), the background estimate Y (dash-dot blue), the decision threshold γ (dashed red), all superimposed on the magnitude of the normalized signal (green).

EWMA, which which the signal variance, s^2. Eighth, the square root of s^2 approximates the standard deviation, s.

Since background noise varies over large timescales, a CFAR detector is used to provide an adaptive decision threshold, γ. The detector decides

$$H = \begin{cases} H_0 & \text{if } X \leq \gamma \\ H_1 & \text{if } X > \gamma \end{cases}$$

where γ is computed

$$\gamma = \alpha s + Y \tag{9}$$

where the value of α is the one that satisfies

$$P_{FA} = 1 - \int_{-\infty}^{\alpha} \frac{1}{\sqrt{2\pi}} e^{-\frac{1}{2}x^2} dx \tag{10}$$

for a required false alarm rate, P_{FA}.

The results of applying these signal processing steps to the a sample signal can be seen in Figure 8. Whenever the solid black line is greater than the dashed red line, a detection event occurs. Notice that a false alarm occurs near sample number 3×10^3 and one almost occurs near 4.3×10^4. The choice of filter parameters and α greatly affects the performance of the system.

Unfortunately, the CFAR detector is not immune to clutter noise like fluttering leaves or heavy rain. The types of correlated noise and clutter shown in Figure 7 occur frequently in practice and must be addressed. Our goal here is not to address these problems because they are application-specific and depend on the acceptable false alarm rate, P_{FA}, and the required detection rate, P_D, for a given application. More generally, the parameters of the EWMA filter must be tuned to be small enough that the detector is agile but large enough that the detector is stable in the presence of noise.

Variations in individual sensors or battery levels can also affect the signal statistics across different sensors or on the

same sensor over time. In our case, the UWB radar sensors are powered from a DC boost regulator which maintains a constant output voltage even when the input battery voltage sags. However, there is no such boost regulator for the processor or its ADC voltage reference. As a result, when the battery voltage sags, both the bias point and signal of the UWB radar sensor appear to increase.

6. RELATED WORK

There has been considerable interest in using UWB radar for a variety of commercial and security application that require detection and ranging capabilities. However, broad use of UWB radar has been largely absent in sensor network applications. In this section, we briefly review some recent sensor network applications, the sensors which they used, the drawbacks with those sensor, and the benefits which could have accrued from the use of UWB radar.

Sharp et al. describe a pursuer-evader game (PEG) in which a sensor network detects the presence and motion of an evader passing through the network and then dispatches a pursuer to track and capture the evader [12]. The PEG node, designed for this application, includes a magnetometer to measure local disturbances to the ambient magnetic field as an evader passes by the node. The authors reported sensing range concerns with their nodes which led to the use of rare-earth magnets on the evaders to enhance detectability. While this approach is fine for demonstrations, in practice, evaders may be much more difficult to tag. The short range of these sensors also led to a high deployment density with nodes placed on a square grid with two meter spacing (100 nodes were deployed in a 400 square meter area). The PEG application could have benefitted from a UWB radar sensor in several ways. First, radar would have obviated the need to tag the evaders. Second, as an active rather than passive technology, UWB radar has a larger sensing radius than magnetic sensors and consequently UWB radar can be deployed in lower densities. Third, radar would have provided direct velocimetry capability, which could be used to improve tracking and pursuit. Like PEG, the VigilNet [8] application also used magnetometers to detect passing vehicles and could have benefitted from using radar.

Arora et al. describe ExScal [3], an extreme-scale sensor network for target detection, classification, and tracking. The ExScal application used a multi-modal sensor node for detection and classification of civilians, soldiers, and vehicles. The eXtreme Scale Mote (XSM) [4], designed specifically for the ExScal application, include passive infrared (PIR), magnetometer, and microphone sensors. The PIR sensors are used to detect all of the target classes and is the only sensor that consistently detects people. However, PIR has some drawbacks as well. First, PIR sensors require a direct line-of-sight to the target. To accomodate this requirement, the XSM includes clear "windows" that allow infrared signals to pass through the enclosure body. More generally, the line-of-sight requirement precludes embedding or concealing the sensors inside of trees, rocks, or other objects which are impervious to light. In addition, the sensitivity of PIR is dependent on the temperature difference between the target and the environment. In hot weather, the sensitivity of the PIR sensor decreases but the UWB radar remains largely unaffected, making radar better suited to warmer climates and outdoor area that receive direct sunlight.

Several earlier papers have considered signal processing on sensor network devices. Li et al. explored detection and classification of large, heavy, and loud military vehicles using acoustic and seismic sensors [11]. Their work used more powerful sensors nodes than those that are typically classified as "mote-class." A significant difference is that their sensors could not detect people. More generally, acoustic sensors require exposure to the environment, potentially compromising their stealth and seismic sensors must often be staked into the ground, constraining their placement. Since UWB radar requires neither exposure to the environment like acoustic sensors nor staking into the ground like seismic sensors, radar offers improved stealthiness and greater deployment flexibility.

A recent study exploring lightweight detection and classification algorithms used nearly identical algorithms as the ones we present [7]. The two key distinctions between this earlier work and ours are: (i) the earlier work focused on different sensing modalities than radar – acoustic, magnetic, and passive infrared; and (ii) the purpose of the paper was to explore lightweight signal processing but not to present a new platform. We are encouraged by this work since it also demonstrates successful signal processing techniques on mote-class devices.

7. CONCLUSIONS

We present the theory, design, and implementation of the Radar Mote, a new sensor network platform that can detect moving objects like people and vehicles using ultrawideband (UWB) radar signals. Unlike passive infrared sensors which do not work if the line of sight to an object is occluded, UWB radar can be embedded in rocks or trees, making them ideal for stealthy surveillance deployments. We provide a number of signal traces illustrating the sensors response to people walking and running past it, as well as vehicles driving by it. While traditional radar signal processing techniques are too complex for mote-class devices, we demonstrate the feasibility of processing radar signals on motes using simple algorithms. Our implementation is quite limited in its scope and evaluation, but its main contribution is that it demonstrates the integration of radar and motes is possible. We expect future work will characterize the sensor model in greater detail, evaluate the robustness of signal processing algorithms employed, and explore classification algorithms to discriminate target classes.

8. ACKNOWLEDGMENTS

We would like to thank Sandip Bapat and Vinayak Naik for their assistance collecting sensor data, Mahesh Arumugam for writing the data collection program, and Hui Cao for assistance developing the TinyOS device driver for the radar and power boards. This work was supported by the Defense Advanced Research Projects Agency under grant OSU-RF#F33615-01-C-1901 and the National Science Foundation Graduate Research Fellowship Program.

9. REFERENCES

[1] Advantaca, Inc. *TWR-ISM-002-I Radar: Hardware User's Manual*, 2002.

[2] A. Arora, P. Dutta, S. Bapat, V. Kulathumani, H. Zhang, V. Naik, V. Mittal, H. Cao, M. Demirbas, M. Gouda, Y. Choi, T. Herman, S. Kulkarni, U. Arumugam, M. Nesterenko, A. Vora, and

M. Miyashita. A line in the sand: A wireless sensor network for target detection, classification, and tracking. *Computer Networks*, 46(5):605–634, December 2004.

[3] A. Arora, R. Ramnath, E. Ertin, P. Sinha, S. Bapat, V. Naik, V. Kulathumani, H. Zhang, H. Cao, M. Sridharan, S. Kumar, N. Seddon, C. Anderson, N. Trivedi, C. Zhang, M. Nesterenko, R. Shah, S. Kulkarni, M. Aramugam, L. Wang, M. Gouda, Y. Choi, D. Culler, P. Dutta, C. Sharp, G. Tolle, M. Grimmer, B. Ferriera, and K. Parker. Exscal: Elements of an extreme scale wireless sensor network. *IEEE RTCSA*, 2005.

[4] P. Dutta, M. Grimmer, A. Arora, S. Bibyk, and D. Culler. Design of a wireless sensor network platform for detecting rare, random and ephemeral events. *IEEE IPSN*, 2005.

[5] B. F. (Ed.). Micropower impulse radar. *Science & Technology Review*, pages 16–29, Jan. 1996.

[6] D. Gay, P. Levis, R. von Behren, M. Welsh, E. Brewer, and D. Culler. The nesc language: A holistic approach to networked embedded systems. In *Proceedings of Programming Language Design and Implementation (PLDI) 2003*, 2003.

[7] L. Gu, D. Jia, P. Vicaire, and et al. Lightweight detection and classification for wireless sensor networks in realistic environments. *In Proceedings of the Third ACM Conference on Embedded Networked Sensor Systems (SenSys)*, nov 2005.

[8] T. He, S. Krishnamurthy, L. Luo, T. Yan, L. Gu, R. Stoleru, G. Zhou, Q. Cao, P. Vicaire, J. A. Stankovic, T. F. Abdelzaher, J. Hui, and B. Krogh. Vigilnet: An integrated sensor network system for energy-efficient surveillance. *ACM Transactions on Sensor Networks*, 2005.

[9] J. Hill. A software architecture supporting networked sensors. *Master's thesis, U.C. Berkeley Dept. of Electrical Engineering and Computer Sciences*, 2000.

[10] J. Hill and D. Culler. Mica: A wireless platform for deeply embedded networks. *IEEE Micro*, 22(6):12–24, 2002.

[11] D. Li, K. Wong, Y. H. Hu, and A. Sayeed. Detection, classification and tracking of targets in distributed sensor networks. *IEEE Signal Processing Magazine*, 19(2), mar 2002.

[12] C. Sharp, S. Schaffert, A. Woo, N. Sastry, C. Karlof, S. Sastry, and D. Culler. Design and implementation of a sensor network system for vehicle tracking and autonomous interception. *IEEE EWSN*, 2005.